Evidence that zymogen granules do not function as an intracellular Ca^{2+} store for the generation of the Ca^{2+} signal in rat parotid acinar cells

Akihiro NEZU*, Akihiko TANIMURA*, Takao MORITA*, Kazuharu IRIE†, Toshihiko YAJIMA† and Yosuke TOJYO*[1]

*Department of Dental Pharmacology, School of Dentistry, Health Sciences University of Hokkaido, Ishikari-Tobetsu, Hokkaido 061-0293, Japan, and †Department of Oral Anatomy, School of Dentistry, Health Sciences University of Hokkaido, Ishikari-Tobetsu, Hokkaido 061-0293, Japan

Rat parotid acinar cells lacking zymogen granules were obtained by inducing granule discharge with the β-adrenoceptor agonist isoproterenol. To assess whether zymogen granules are involved in the regulation of Ca^{2+} signalling as intracellular Ca^{2+} stores, changes in cytosolic free Ca^{2+} ion concentration ($[Ca^{2+}]_i$) were studied with imaging microscopy in fura-2-loaded parotid acinar cells lacking zymogen granules. The increase in $[Ca^{2+}]_i$ induced by muscarinic receptor stimulation was initiated at the apical pole of the acinar cells, and rapidly spread as a Ca^{2+} wave towards the basolateral region. The magnitude of the $[Ca^{2+}]_i$ response and the speed of the Ca^{2+} wave were essentially similar to those in control acinar cells containing zymogen granules. Western blot analysis of the inositol 1,4,5-trisphosphate receptor (IP_3R) was performed on zymogen granule membranes and microsomes using anti-IP_3R antibodies. The immunoreactivity of all three IP_3Rs was clearly observed in the microsomal preparations. Although a weak band of IP_3R type-2 was detected in the zymogen granule membranes, this band probably resulted from contamination by the endoplasmic reticulum (ER), because calnexin, a marker protein of the ER, was also detected in the same preparation. Furthermore, Western blotting and reverse transcriptase-PCR analysis failed to provide evidence for the expression of ryanodine receptors in rat parotid acinar cells, whereas expression was clearly detectable in rat skeletal muscle, heart and brain. These results suggest that zymogen granules do not have a critical role in Ca^{2+} signalling in rat parotid acinar cells.

Key words: Ca^{2+} mobilization, inositol 1,4,5-trisphosphate (IP_3) receptor, intracellular Ca^{2+} store, ryanodine receptor.

INTRODUCTION

Stimulation of plasma membrane receptors coupled with activation of phospholipase C causes Ca^{2+} mobilization from intracellular Ca^{2+} stores via the formation of inositol 1,4,5-trisphosphate (IP_3). The endoplasmic reticulum (ER) is well established as a primary Ca^{2+} store involved in the IP_3-induced Ca^{2+} mobilization, but whether other cytoplasmic organelles participate as Ca^{2+} stores in Ca^{2+} signalling remains unclear [1], although mitochondria have been reported to modulate Ca^{2+} signalling via Ca^{2+} uptake and Ca^{2+}-induced Ca^{2+} release [2,3].

In exocrine acinar cells, including parotid acinar cells, the agonist-induced Ca^{2+} release from intracellular Ca^{2+} stores is usually initiated in the apical pole of the cell, and then propagates towards the basolateral region [4–7]. The Ca^{2+} mobilization induced by low concentrations of agonists is predominant in the apical region, rather than in the basolateral region. Although the molecular mechanism underlying the polarized Ca^{2+} signal is not clear, it has been suggested that the apical region of acinar cells has a particularly high sensitivity to IP_3 [8,9]. Zymogen (secretory) granules are localized in the apical region, and are known to have a high Ca^{2+} content [10,11], and Marty [12] speculated that the zymogen granules may be a physiological Ca^{2+} store in exocrine acinar cells. This hypothesis has been supported by the finding [13] that IP_3 and a putative Ca^{2+}-releasing messenger, cyclic ADP-ribose (cADPr), could cause Ca^{2+} release from isolated pancreatic zymogen granules. However, Yule et al. [14] have reported that pancreatic zymogen granules, highly purified on a Percoll gradient, are insensitive to IP_3. In addition, immunocytochemical studies have shown that IP_3 receptors (IP_3Rs) are expressed in a restricted space of the apical pole [14–16], which does not correlate with the localization of zymogen granules. Thus the role of zymogen granules in the generation of agonist-induced Ca^{2+} signals remains to be fully explained.

Amylase release from rat parotid acinar cells is induced primarily by stimulation of β-adrenoceptors. Intraperitoneal injection of the β-adrenoceptor agonist isoproterenol caused, within the space of an hour, the discharge of more than 90 % of the total amylase, which had been accumulated in rat parotid glands [17], and the acinar cells obtained from isoproterenol-injected rats would be expected to lack zymogen granules. To assess whether zymogen granules make a significant contribution to the generation of intracellular Ca^{2+} signalling, the pattern of Ca^{2+} mobilization in parotid acinar cells obtained from isoproterenol-injected rats was analysed. In addition to IP_3, isolated pancreatic zymogen granules have been reported to respond to cADPr [13]. As cADPr is believed to induce Ca^{2+} mobilization via its action on the ryanodine receptor (RyR) [18], we examined further the expression of IP_3R and RyR in rat parotid acinar cells using Western blot analysis and reverse transcriptase (RT)-PCR.

MATERIALS AND METHODS

Chemicals

Carbachol, isoproterenol, trypsin (type III), soya-bean trypsin inhibitor, collagenase and BSA were purchased from Sigma

Abbreviations used: AM, acetoxymethyl ester; $[Ca^{2+}]_i$, cytosolic free Ca^{2+} ion concentration; cADPr, cyclic ADP-ribose; ER, endoplasmic reticulum; IP_3(R), inositol 1,4,5-trisphosphate (receptor); RT, reverse transcriptase; RyR, ryanodine receptor.

[1] To whom correspondence should be addressed (e-mail tojyo@hoku-iryo-u.ac.jp).

(St Louis, MO, U.S.A.). Fura-2 [acetoxymethyl ester (AM)], fluo-3 AM, EGTA and Hepes were from Dojin Laboratories (Kumamoto, Japan). Lyso Tracker Red DND-99 was from Molecular Probes (Eugene, OR, U.S.A.). PMSF, pepstatin A, leupeptin and dithiothreitol were purchased from Wako Pure Chemicals (Osaka, Japan). Tosyl-L-phenylalanylchloromethane ('TPCK') was obtained from Roche Molecular Biochemicals (Mannheim, Germany). Horseradish-peroxidase-conjugated goat anti-rabbit IgG was purchased from Pierce (Rockford, IL, U.S.A.). Horseradish-peroxidase-conjugated goat anti-mouse IgG was from Biosource International (Camarillo, CA, U.S.A.). The polyclonal anti-IP_3R antibodies were raised against C-terminal peptides specific for each of the three IP_3R subtypes [19]. Monoclonal antibody 34C, which recognizes all three mammalian RyR isoforms [20], was from Affinity BioReagents Inc. (Golden, CO, U.S.A.). Anti-calnexin monoclonal antibody was purchased from Transduction Laboratories (Lexington, KY, U.S.A.).

Protein concentration was measured with the bicinchoninic acid protein assay system (Pierce).

Preparation of parotid acinar cells

Parotid acinar cells were prepared from male Wistar strain rats (200–300 g) using trypsin and collagenase, as described elsewhere [21]. Dispersed acinar cells were finally suspended in a Hanks balanced salt solution buffered with 20 mM Hepes/NaOH, pH 7.4 (HBSS-H) containing 0.1 % (w/v) BSA.

In order to obtain acinar cells lacking zymogen granules, rats were intraperitoneally injected with isoproterenol (30 mg/kg) and killed 90–120 min later. Dispersed acinar cells were prepared as described above. The amylase contents of dispersed acinar cells was measured using the method of Bernfeld [22].

Preparation of parotid zymogen granules

Rat parotid glands were minced finely, and rinsed in ice-cold buffer A [10 mM Hepes/NaOH (pH 6.8)/0.1 mM $MgSO_4$/3 mM ATP/250 mM sucrose/0.2 mM PMSF/1 mM dithiothreitol/10 μM leupeptin/0.1 mM tosyl-L-phenylalanylchloromethane/10 μM pepstatin A/0.1 mg/ml soya-bean trypsin inhibitor]. The minced tissue was homogenized in buffer A using a Teflon/glass homogenizer. The homogenate was centrifuged at 150 ***g*** for 5 min, and the supernatant was centrifuged further at 1500 ***g*** for 10 min. The pellet was mixed with buffer A containing 50 % (v/v) Percoll and centrifuged at 20000 ***g*** for 20 min. After centrifugation, the white pellet was collected from the bottom of the tube, resuspended in buffer A without Percoll and 'washed' by three successive centrifugations of 10 min at 1500 ***g***. The pellet was finally centrifuged at 150 ***g*** for 5 min to remove contaminating erythrocytes, and suspended in fresh buffer A.

Preparation of granule membranes

The prepared zymogen granules were disrupted for 5 min in a sonicator bath (model 2510J-MT; Branson Ultrasonic Corp., Danbury, CT, U.S.A.). By observation with light microscopy, we confirmed that the sonication resulted in complete disruption of the zymogen granules. The disrupted granules were centrifuged at 100000 ***g*** for 60 min, and the resulting membrane fraction was resuspended in buffer A. The membrane preparation was stored at −80 °C until use.

Preparation of microsomal membranes

Parotid glands, whole brain, heart and femoral skeletal muscle were excised from male rats and minced straight afterwards. The minced tissue was rinsed with HBSS-H and homogenized with a Polytron homogenizer in ice-cold buffer A (60 s). The homogenates were centrifuged at 1500 ***g*** for 10 min, and the supernatant was centrifuged further at 100000 ***g*** for 60 min. The resulting microsomal fractions were resuspended in buffer A and stored at −80 °C until use.

Electrophoresis and Western blot analysis

Samples were subjected to electrophoresis on 3–8 % NuPAGE Tris-acetate gels (Novex, San Diego, CA, U.S.A.) and transferred to nitrocellulose membranes (Schleicher & Schuell, Keene, NH, U.S.A.). Detection of IP_3Rs was performed as described previously [19] using the polyclonal anti-IP_3R antibodies and horseradish-peroxidase-conjugated goat anti-rabbit IgG. For detection of RyRs and calnexin, nitrocellulose membranes were blocked for 1 h in Tris-buffered saline containing 5 % (w/v) skimmed milk powder, and then incubated for 2 h with antibody raised against RyRs (34C; 1:5000 dilution) and anti-calnexin antibody (1:1000 dilution) in Tris-buffered saline containing 5 % skimmed milk powder. Blots were then incubated for 1 h with horseradish-peroxidase-conjugated anti-mouse IgG in Tris-buffered saline containing 5 % skimmed milk powder. Immunoreactive bands were visualized by ECL® (Amersham Biosciences, Little Chalfont, Bucks., U.K.).

RT-PCR analyses of RyRs

The excised tissues were homogenized in TRIzol reagent (Gibco BRL, Life Technologies, Rockville, MD, U.S.A.) with a Polytron homogenizer, and total RNAs were extracted from the tissues according to the manufacturer's protocol. First-strand cDNA was synthesized from 1 μg of each RNA sample using oligo-dT_{16} primer (Roche Molecular Biochemicals) and RT (ReverTra Ace; Toyobo, Osaka, Japan). The primers used in RT-PCR analysis were as follows: common to RyRs type-1 and -3, 5′-GGGACAAGTTTGTCAAGCGGAAGGT-3′ (forward) and 5′-CGGACGCCCACATACATGTGGAA-3′ (reverse); specific for RyR type-2, 5′-GGGAGAGACAGAATCAGCGAGTTAC-3′ (forward) and 5′-CGGACGCCCACATACATGTGGAA-3′ (reverse). A 1 μl aliquot of RT product was subjected to PCR amplification. Following an initial denaturation step for 10 min at 95 °C, reactions for type-1 and -3 were performed in a Gene Amp PCR system 2400 (PerkinElmer Biosystems, Norwalk, CT, U.S.A.) for 30 cycles, consisting of a denaturation step of 1 min at 94 °C, annealing for 1 min at 48 °C, and extension for 1 min at 72 °C. The final extension step was for 7 min at 72 °C. The reactions for type 2 were the same as those for types-1 and -3, except that the annealing temperature was 58 °C. The primers and conditions for the RT-PCR analysis of glyceraldehyde-3-phosphate dehydrogenase were as described previously [23]. The PCR products were electrophoretically fractionated on 2 % (w/v) agarose gels (Takara, Tokyo, Japan), and DNA was stained with ethidium bromide for fluorescence detection.

Digestion of the PCR products using the restriction enzymes *Eco*RV (Roche Molecular Biochemicals), *Hin*cII and *Bgl*II (Toyobo, Osaka, Japan) were performed at 37 °C for 1 h.

Imaging of cytosolic free Ca^{2+} ion concentration ($[Ca^{2+}]_i$)

Dispersed parotid acinar cells were loaded with 2 μM fura-2 AM or 1 μM fluo-3 AM for 45 min at room temperature (25 ± 3 °C). The dye-loaded cells were attached to a Cell-Tak-coated glass coverslip at the bottom of a small recording chamber. The fura-2 fluorescence images were acquired as described elsewhere [7] using an Argus HiSCA imaging system (Hamamatsu Photonics,

Shizuoka, Japan) attached to an inverted fluorescence microscope (Diaphot; Nikon Inc., Tokyo, Japan). The fluorescence ratio was converted into $[Ca^{2+}]_i$, and the digital imaging of $[Ca^{2+}]_i$ was displayed as 'pseudo-colour'. Fluo-3 fluorescence was observed using a confocal laser scanning microscope (Leica TCS-SP system; Leica, Heidelberg, Germany) equipped with a $40 \times$ PL Fluotar objective. Images of fluo-3 fluorescence were obtained by using an excitation wavelength of 488 nm, and emission was monitored over 490–560 nm.

Staining of secretory granules with Lyso Tracker Red DND-99

For the staining of zymogen granules, dispersed parotid acinar cells were incubated in HBSS-H containing 100 nM of Lyso Tracker Red DND-99 (a specific stain for acidic organelles) for 2 min at room temperature. Fluorescence from the stained cells was detected with a confocal laser scanning microscope (Leica TCS-SP system). The confocal images were captured using an excitation wavelength of 568 nm, and emission was monitored over 580–650 nm.

Immunocytochemistry of IP_3Rs

Dispersed parotid acinar cells were fixed with 4 % (w/v) paraformaldehyde in 0.1 M phosphate buffer, pH 7.4, for 2 h at 4 °C. After washing with 0.01 M PBS, the cells were permeabilized with 40 μg/ml saponin in PBS and blocked with PBS containing 1.5 % (v/v) goat serum and 1 % (w/v) BSA for 60 min at room temperature. The cells were then incubated with antibodies raised against IP_3R type-2 (1.2 μg/ml) and type-3 (0.6 μg/ml) for 60 min. After washing, the cells were incubated for 60 min with FluoroLink™ Cy™3-conjugated goat anti-rabbit IgG (Amersham Biosciences). Fluorescence was detected with a Leica TCS-SP confocal microscope.

Electron microscopy

Isolated zymogen granules were fixed successively with 2 % (w/v) paraformaldehyde/2 % (v/v) glutaraldehyde and 1 % (w/v) osmium tetroxide, dehydrated in an ethanol series and embedded in Epon 812. Sections cut with an ultramicrotome were doubly stained with uranyl acetate and lead citrate, and observed under a Hitachi H-500 electron microscope.

RESULTS

Measurement of amylase content and staining with Lyso Tracker Red

To confirm that most of the amylase accumulated in parotid glands was discharged by isoproterenol injection, dispersed acinar cells were stained with Lyso Tracker Red DND-99, a specific stain for acidic organelles. The acinar cells isolated from control rats contained many zymogen granules stained brightly with this dye (Figure 1A, lower panel labelled 'b'), whereas much less fluorescence was observed in the acinar cells from the isoproterenol-injected rats (Figure 1B, lower panel labelled 'b'). Furthermore, the content of amylase was estimated by determining the amylase activities in the homogenates of dispersed acinar cells. The values were decreased to 6.4 ± 2.3 % (mean $\pm$ S.E.M.; $n = 4$) of the control values within 2 h after isoproterenol injection. These results indicate that injection with a high dose of isoproterenol is effective in leading to an absence of zymogen granules in acinar cells.

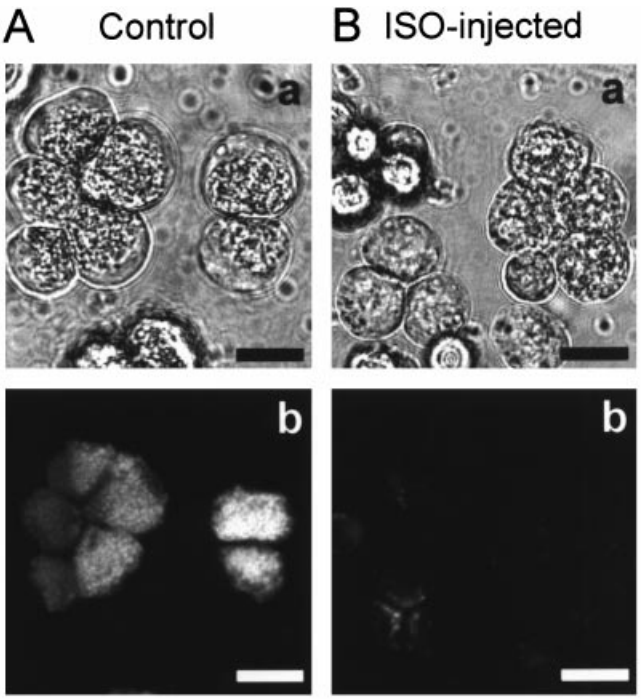

Figure 1 Dispersed rat parotid acinar cells obtained from control (A) and isoproterenol (ISO)-injected (B) rats

Transmission images (upper panels labelled 'a') and the corresponding confocal images (lower panels labelled 'b') of acinar cells stained with Lyso Tracker Red DND-99. Acinar cells were incubated for 2 min with fluorescent stain (100 nM). Bars indicate 10 μm.

Ca^{2+} imaging in parotid acinar cells from isoproterenol-injected rats

The fura-2-loaded acinar cells were stimulated with 10 μM carbachol in Ca^{2+}-free medium containing 0.2 mM EGTA, and changes in $[Ca^{2+}]_i$ were monitored with the Argus HiSCA imaging system (Figure 2). In control acinar cells, the rise in $[Ca^{2+}]_i$ was initiated at the apical pole at approx. 0.4 sec after stimulation, before spreading rapidly as a Ca^{2+} wave towards the basolateral region (Figure 2A). A similar pattern of increases in $[Ca^{2+}]_i$ was observed in the acinar cells isolated from isoproterenol-injected rats (Figure 2C). The time-dependent changes in $[Ca^{2+}]_i$ were monitored for selected areas of interest in the apical and basal poles of each acinar cell (Figures 2B and 2D), and both the maximal $[Ca^{2+}]_i$ and the time ($t_{1/2}$) required to attain 50 % of the maximum increase in $[Ca^{2+}]_i$ were quantitatively evaluated from the time courses of the changes in $[Ca^{2+}]_i$ following stimulation with 1 and 10 μM carbachol (Table 1). No significant differences in either the magnitude of $[Ca^{2+}]_i$ or the speed of the increase in $[Ca^{2+}]_i$ were found between acinar cells from the control and isoproterenol-injected rats.

We subsequently performed both Ca^{2+} imaging and Lyso Tracker Red staining on the same acinar cells using a confocal microscope. The Ca^{2+} images obtained using fluo-3 confirmed that carbachol stimulation caused Ca^{2+} waves in parotid acinar cells (Figure 3). The polarized pattern of Ca^{2+} signal observed in the acinar cells from the isoproterenol-injected rats (Figure 3B) was essentially similar to that observed in the control cells (Figure 3A). After Ca^{2+} imaging, the same cells were stained with Lyso Tracker Red. The staining showed that the acinar cells isolated from the isoproterenol-injected rats lacked zymogen

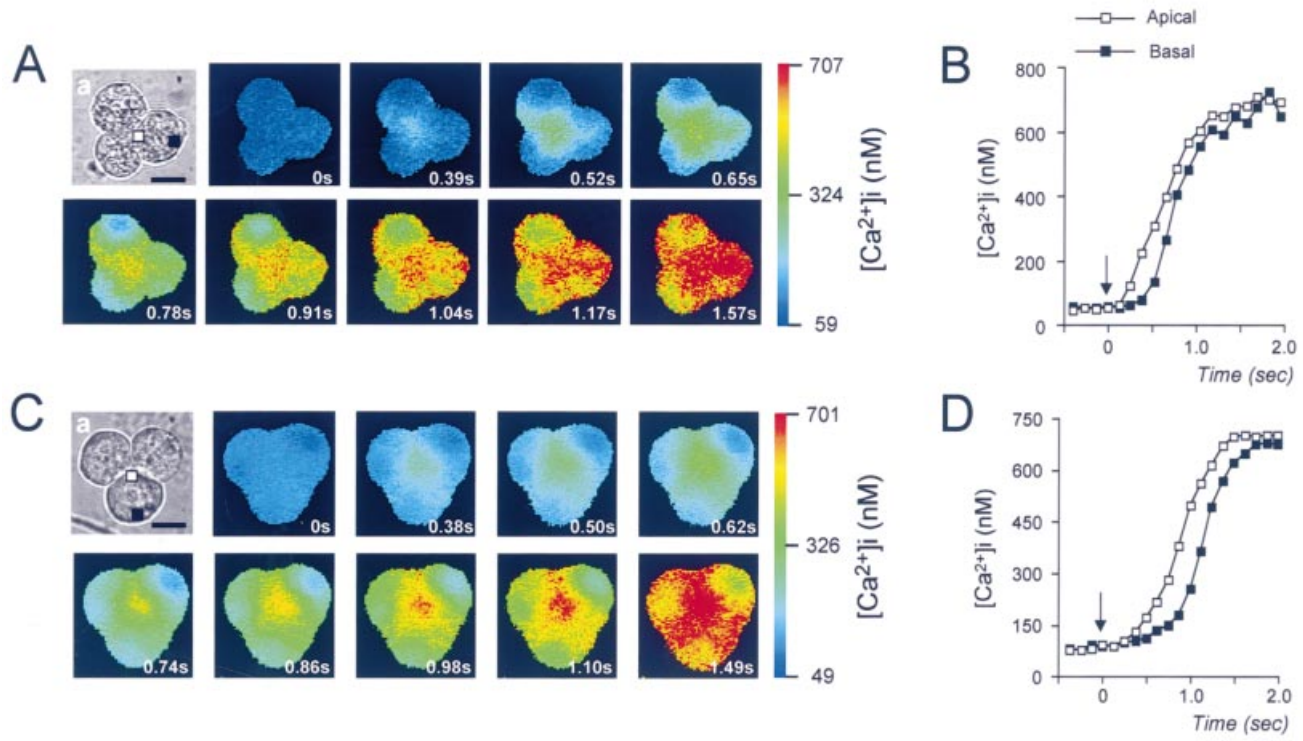

Figure 2 Ca^{2+} waves induced by carbachol in parotid acinar cells from control (A and B) and isoproterenol-injected (C and D) rats

The fura-2-loaded cells were stimulated with 10 μM carbachol in Ca^{2+}-free medium containing 0.2 mM EGTA. (**A** and **C**) Ca^{2+} images expressed as 'pseudo'-colour. Panels labelled 'a' show transmission images; the scale bars therein represent 10 μm. The time after addition of carbachol is shown in the bottom right-hand corner of each coloured panel of **A** and **C**. (**B** and **D**) Time courses of changes in $[Ca^{2+}]_i$ taken from the open squares shown in the transmission images (panels 'a') from **A** and **C**. The arrows indicate the time of addition of carbachol.

Table 1 Magnitude and speed of the increases in $[Ca^{2+}]_i$ induced with 1 or 10 μM carbachol (CCh) in parotid acinar cells from control and isoproterenol (ISO)-injected rats

Time-dependent changes in $[Ca^{2+}]_i$ at the apical and basal poles of each cell were measured, and the maximal $[Ca^{2+}]_i$ (Max $[Ca^{2+}]_i$) and the time ($t_{1/2}$) required to reach 50% of the maximal $[Ca^{2+}]_i$ were determined. Values are means $\pm$ S.E.M. for measurements in 11–13 cells. The resting $[Ca^{2+}]_i$ before CCh stimulation was 78 $\pm$ 2 nM.

	Max $[Ca^{2+}]_i$ (nM)		$t_{1/2}$ (s)	
CCh added (μM) ...	1	10	1	10
Apical pole				
Control	337 $\pm$ 36	594 $\pm$ 49	1.63 $\pm$ 0.25	0.75 $\pm$ 0.05
ISO-injected	360 $\pm$ 28	549 $\pm$ 38	1.80 $\pm$ 0.15	0.90 $\pm$ 0.07
Basal pole				
Control	270 $\pm$ 25	479 $\pm$ 36	1.92 $\pm$ 0.27	0.92 $\pm$ 0.04
ISO-injected	287 $\pm$ 22	499 $\pm$ 47	2.05 $\pm$ 0.17	1.03 $\pm$ 0.06

granules (Figure 3B, 'LTR'), although the control cells contained many granules (Figure 3A, 'LTR').

Western blot analysis of IP_3Rs

Zymogen granules and microsomes were prepared as described in the Materials and methods section. Figure 4 shows an electron micrograph of the zymogen granules prepared by centrifugation on a Percoll gradient. Although the obtained zymogen granules were highly purified, the preparation was slightly contaminated by non-granule membranes. Immunoblot analysis (Figure 5) was performed on zymogen granules and microsomes from parotid acinar cells using three antibodies specific for the IP_3R subtypes, i.e. types 1, 2 and 3 [19]. None of the IP_3Rs were detected in the zymogen granule preparation (Figure 5B), whereas the immunoreactive bands pertaining to the presence of IP_3Rs were visualized in the microsomal membranes, the most intense band coinciding with the IP_3R type-2 antibody and less intense bands being observed for the IP_3R type-1 and -3 antibodies (Figure 5A). To remove the influence of soluble proteins contained in zymogen granules, we disrupted the zymogen granules completely by sonication and collected the membranes by ultracentrifugation. This process was expected to lead to an enrichment of the granule membrane proteins. When the membrane preparation was subjected to Western blot analysis, a weak immunoreactive band of the IP_3R type-2, but not types 1 and 3, was observed (Figure 5C). Since there was a possibility that the weak signal of type-2 reflected the presence of contaminants, we probed for the presence of calnexin, a 90 kDa protein known to be localized exclusively to the ER [24], by immunoblotting with anti-calnexin antibody (Figure 5D). A weak immunoreactivity was detected in the granule membrane preparation (Figure 5D, lane 2), although the intensity of the reactive band was much less than that obtained with the microsomal preparation (Figure 5D, lane 1).

Immunocytochemistry of IP_3Rs

If IP_3Rs are expressed on zymogen granules, then amylase exocytosis might result in the redistribution of IP_3Rs. To assess

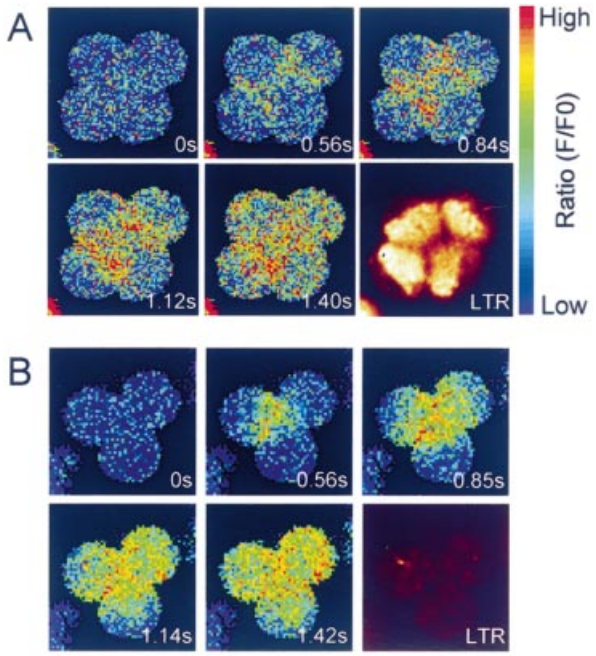

Figure 3 Confocal images of fluo-3 fluorescence in parotid acinar cells from control (A) and isoproterenol-injected (B) rats

The fluo-3-loaded cells were stimulated with 10 μM carbachol in Ca^{2+}-free medium containing 0.2 mM EGTA. Ratio images were represented as relative fluorescence intensity (F/F_0). The time after addition of carbachol is shown in the bottom right-hand corner of each panel. After the recording of fluo-3 fluorescence, the same cells were stained with Lyso Tracker Red DND-99 (LTR).

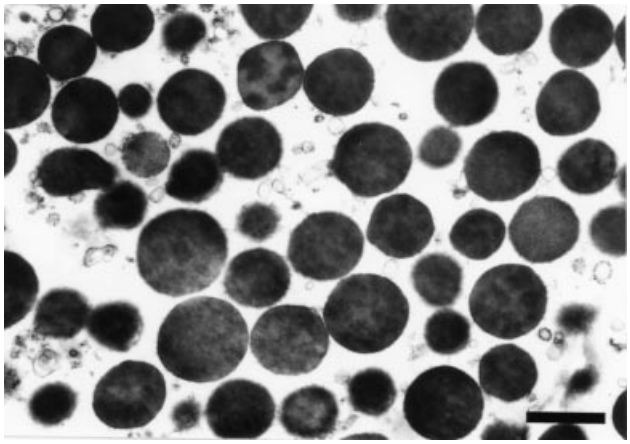

Figure 4 Electron micrograph of a zymogen granule preparation from rat parotid glands

Granules were purified by Percoll-gradient centrifugation. The bar represents 1 μm.

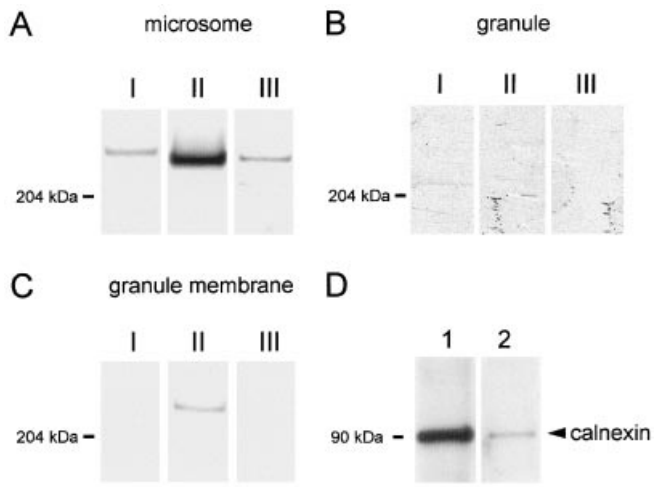

Figure 5 Immunoblot analyses of IP_3Rs (A, B and C) and calnexin (D) in microsomes and zymogen granules prepared from rat parotid glands

(**A**–**C**) For detection of IP_3Rs, 10 μg of protein from (**A**) the microsomal preparation, (**B**) zymogen granules or (**C**) the membrane preparation of zymogen granules were electrophoresed on 3–8% NuPAGE gels, transferred on to a nitrocellulose membrane and probed with anti-IP_3R type-1 (lanes I), type-2 (lanes II) and type-3 (lanes III) antibodies. (**D**) For detection of calnexin, 30 μg of the protein was electrophoresed, transferred and probed with anti-calnexin antibody. Lane 1: microsomes; lane 2, the granule membrane preparation.

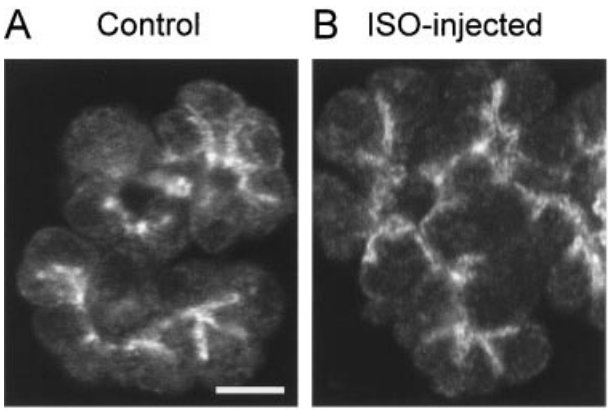

Figure 6 Immunofluorescence localization of IP_3R type-2 in parotid acinar cells from control (A) and isoproterenol-injected (B) rats

Dispersed acinar cells were stained with the IP_3R type-2 antibody and imaged by confocal mycroscopy. The bar represents 10 μm.

this possibility, we investigated the localization of IP_3Rs by immunocytochemistry. Immunofluorescence using the IP_3R type-2 antibody showed that the IP_3R type-2 was localized predominantly to the regions close to the luminal and lateral membranes (Figure 6). No significant differences in the distribution of signals were found between the acinar cells from the control and isoproterenol-injected rats, indicating that amylase exocytosis did not change the distribution of IP_3Rs. Similar results were also obtained by immunocytochemistry using type-3 antibody (results not shown).

Western blot and RT-PCR analysis of RyR subtypes

Immunoblot analysis of RyRs was performed on the microsomal membranes from several different tissues and the parotid zymogen granule membrane using the monoclonal antibody 34C, which recognizes all three mammalian RyR subtypes. As shown in Figure 7(A), RyR was clearly detected in microsomes from skeletal muscle, heart and brain, whereas no immunoreactive band was found in the microsomes from the parotid gland and

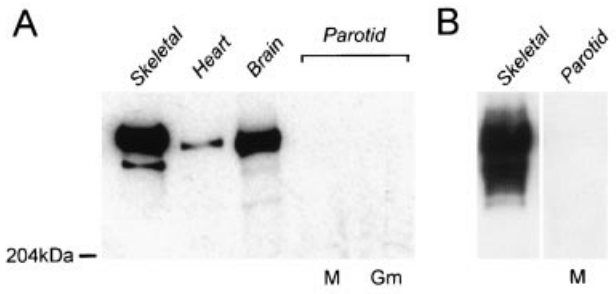

Figure 7 Immunoblot analysis of RyRs in microsomes from different tissues and zymogen granule membranes

Microsomes were prepared from skeletal muscle, heart, brain and the parotid glands. Samples containing 30 μg (**A**) or 100 μg (**B**) of proteins were electrophoresed on 3–8% NuPAGE gels, transferred on to a nitrocellulose membrane and probed with an anti-RyR antibody (34C). M, parotid microsomes; Gm, granule membrane.

zymogen granule membranes. Even when a 3-fold-larger sample of parotid microsomes was subjected to electrophoresis, no active band of RyR was identified (Figure 7B).

To examine the expression of mRNAs for RyR subtypes in rat parotid acinar cells, RT-PCR analysis was performed as described in the Materials and methods section. When amplified with the primers common to RyR types-1 and -3, an RT-PCR product of the expected size (approx. 530-bp) was clearly detected in skeletal muscle and the brain; less well so in the heart (Figure 8A). When total RNA extracted from whole parotid tissue was used, a faint band of PCR product was detected (Figure 8A, lane 5). However, when total RNA was extracted from dispersed parotid acinar cells, no PCR product was generated using the primers for RyR types-1 and -3 (Figure 8A, lane 4). PCR analysis using the primers for RyR type-2 clearly showed a product of the predicted size (approx. 490 bp) in the heart and brain (Figure 8B, lanes 2 and 3), but there was little or no detectable PCR product in skeletal muscle, parotid acinar cells and whole parotid tissue (Figure 8B, lanes 1, 4 and 5). The PCR products from skeletal muscle, brain and the heart were digested using the restriction enzymes *Eco*RV, *Hinc*II and *Bgl*II to identify RyR types-1, -2 and -3 respectively, and the products were confirmed to correspond to the RyRs (results not shown).

DISCUSSION

The present study found that there was little or no difference in the pattern of carbachol-induced Ca^{2+} signalling between the acinar cells of rat parotid glands isolated from control and isoproterenol-injected rats. Zymogen granules had been almost completely discharged from the acinar cells on isoproterenol injection, as confirmed by the measurement of accumulated amylase content and staining with the fluorescent probe Lyso Tracker Red. The finding that the absence of zymogen granules did not influence the generation and propagation of the Ca^{2+} wave raises serious doubts about the validity of the concept that zymogen granules have a major role as an intracellular Ca^{2+} store. Ligation of the rat salivary duct is known to cause reversible atrophy of the salivary glands, leading to the disappearance of zymogen granules from acinar cells [25]. Liu et al. [26] demonstrated that there were no significant differences in the magnitude of acetylcholine-induced increases in $[Ca^{2+}]_i$ between acinar cells from control and atrophied parotid glands, suggesting that the presence of zymogen granules is not necessarily required for Ca^{2+} mobilization in rat parotid acinar cells.

The immunoblotting data obtained in the present study did not provide evidence that IP_3Rs are present in parotid zymogen granules. Although a weak immunoreactive band of type-2 IP_3R was detected in the granule membrane preparation, calnexin, an integrated membrane protein of the ER, was also detected faintly in the same sample. As shown by electron microscopy, the zymogen granules purified in this experiment were slightly contaminated by non-granule membranes. These results strongly suggest that the immunoreactive band of IP_3R type-2 results from contamination by microsomal membranes. It is possible that removal of soluble proteins from the granule preparation enriches not only granule membranes, but also non-granule membrane contaminants. Yule et al. [14] have indicated that the

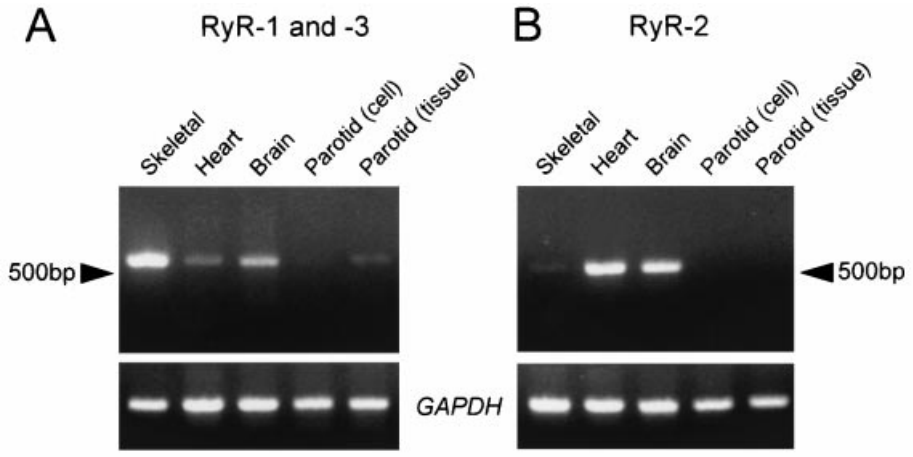

Figure 8 RT-PCR analysis of RyRs in skeletal muscle, heart, brain and parotid gland

In the case of parotid gland, total RNA was extracted from dispersed acinar cells and produced whole-tissue cDNA was amplified by PCR using the primers common to types-1 and -3 (**A**) or the primers specific to type-2 (**B**) as described in the Materials and methods section. The levels of glyceraldehyde-3-phosphate dehydrogenase (GAPDH) shown in the lower panel indicate that approximately similar levels of total RNA had been loaded.

detection of immunoreactive bands for IP_3Rs is dependent on purification of pancreatic zymogen granules. Although our data cannot completely exclude the possibility that a small portion of IP_3Rs is present in parotid zymogen granules, it is reasonable to consider that zymogen granules are unlikely to have a critical role as a IP_3-sensitive Ca^{2+} store in parotid acinar cells.

Using immunogold electron microscopy, several groups have shown that IP_3Rs are present on the secretory granules in insulin-secreting βTC-3 cells [27] and bovine adrenal chromaffin cells [28]. However, since immunocytochemical data ultimately depend on the specificity of the antibody, subcellular localization of immunolabelling should be interpreted with caution. Indeed, the specificity of the antibody used in insulin-secreting βTC-3 cells [27] has been called into question, because the antibody was shown to cross-react with insulin in the secretory granules [29].

In addition to IP_3, isolated pancreatic zymogen granules have been reported to respond to cADPr [13]. However, this is inconsistent with our previous result that cADPr did not evoke Ca^{2+} release from intracellular Ca^{2+} stores in saponin-permeabilized rat parotid acinar cells [30]. Since cADPr is thought to activate RyRs [18], we have assessed whether RyRs exist in rat parotid acinar cells. Western blot analysis using monoclonal antibodies raised against RyRs did not reveal the presence of RyRs in parotid acinar cells. The absence of RyR in parotid acinar cells is supported further by the result that the RT-PCR analysis failed to detect any expression of RyR mRNA. A small amount of PCR product was detected when cDNA was extracted from whole parotid tissue. Since the isolated whole tissue contains blood vessels and connective tissue, in addition to gland tissue, the appearance of the weak PCR band does not necessarily indicate the expression of RyRs in parotid acinar cells.

There are several studies suggesting that RyRs are expressed in the parotid gland. An earlier immunoblot study has shown that the immunoreactive band of RyR type-3 is detected in mouse parotid acini [31], although the signal was much weaker than that in avian pectoralis muscle. Zhang et al. [32] reported that a RyR highly homologous with the RyR type-1 was detected by RT-PCR analysis in rat parotid acinar cells, but it should be noted that the PCR reactions in that study were carried out for 45 cycles (cf. 30 cycles in our study) using a concentration of cDNA template from rat parotid cells that was 10 times higher than that of the brain. It is possible that the apparent discrepancy arises from differences in the reaction conditions for the PCR amplification. More recent work suggested that nitric oxide induced a small release of Ca^{2+} from intracellular ryanodine-sensitive stores in rat parotid acinar cells through a cGMP-mediated process [33], and proposed that the signalling pathway may form the basis for prolonged Ca^{2+}-induced Ca^{2+} release. However, there is no direct evidence showing that the RyRs have an important role in the receptor-mediated Ca^{2+} waves in parotid acinar cells.

The present study does not support the hypothesis that parotid zymogen granules may be involved in the rapid increases in $[Ca^{2+}]_i$ as IP_3- or cADPr-sensitive intracellular Ca^{2+} stores. However, the possibility that the zymogen granules may modulate the regulation of $[Ca^{2+}]_i$ is not excluded, since specific mechanisms for Ca^{2+} uptake into zymogen granules are known to be present in the granular membrane [1,34]. Martinez et al. [35] suggested that the secretory granules in rat submandibular acinar cells are an IP_3-insensitive Ca^{2+} store that releases Ca^{2+} only when the pH gradient across the membrane is collapsed. Although the functional significance of the pH-gradient-dependent Ca^{2+} release is unknown, it is possible that the secretory granules contribute to the intracellular processes of Ca^{2+} homoeostasis as slowly exchanging Ca^{2+} stores [1].

This work was supported by a Grant-in-Aid for Scientific Research (No. 12470391) from the Ministry of Education, Culture, Sports, Science and Technology of Japan. We thank Dr R. James Turner (National Institute of Dental and Craniofacial Research, National Institutes of Health, Bethesda, MD, U.S.A.) for his collaboration in raising anti-IP_3R antibodies.

REFERENCES

1 Pozzan, T., Rizzuto, R., Volpe, P. and Meldolesi, J. (1994) Molecular and cellular physiology of intracellular calcium stores. Physiol. Rev. **74**, 595–636
2 Ichas, F., Jouaville, L. S. and Mazat, J.-P. (1997) Mitochondria are excitable organelles capable of generating and conveying electrical and calcium signals. Cell (Cambridge, Mass.) **89**, 1145–1153
3 Tinel, H., Cancela, J. M., Mogami, H., Gerasimenko, J. V., Gerasimenko, O. V., Tepikin, A. V. and Petersen, O. H. (1999) Active mitochondria surrounding the pancreatic acinar granule region prevent spreading of inositol trisphosphate-evoked local cytosolic Ca^{2+} signals. EMBO J. **18**, 4999–5008
4 Kasai, H. and Augustine, G. J. (1990) Cytosolic Ca^{2+} gradients triggering unidirectional fluid secretion from exocrine pancreas. Nature (London) **348**, 735–738
5 Kasai, H., Li, Y. X. and Miyashita, Y. (1993) Subcellular distribution of Ca^{2+} release channels underlying Ca^{2+} waves and oscillations in exocrine pancreas. Cell (Cambridge, Mass.) **74**, 669–677
6 Thorn, P., Lawrie, A. M., Smith, P. M., Gallacher, D. V. and Petersen, O. H. (1993) Local and global cytosolic Ca^{2+} oscillations in exocrine cells evoked by agonists and inositol trisphosphate. Cell (Cambridge, Mass.) **74**, 661–668
7 Tojyo, Y., Tanimura, A. and Matsumoto, Y. (1997) Imaging of intracellular Ca^{2+} waves induced by muscarinic receptor stimulation in rat parotid acinar cells. Cell Calcium **22**, 455–462
8 Tanimura, A., Matsumoto, Y. and Tojyo, Y. (1998) Polarized Ca^{2+} release in saponin-permeabilized parotid acinar cells evoked by flash photolysis of 'caged' inositol 1,4,5-trisphosphate. Biochem. J. **332**, 769–772
9 Ito, K., Miyashita, Y. and Kasai, H. (1999) Kinetic control of multiple forms of Ca^{2+} spikes by inositol trisphosphate in pancreatic acinar cells. J. Cell Biol. **146**, 405–413
10 Clemente, F. and Meldolesi, J. (1975) Calcium and pancreatic secretion. Subcellular distribution of calcium and magnesium in the exocrine pancreas of the guinea pig. J. Cell. Biol. **65**, 88–102
11 Nakagaki, I., Sasaki, S., Shiguma, M. and Imai, Y. (1984) Distribution of elements in the pancreatic exocrine cells determined by electron probe X-ray microanalysis. Pflügers Arch. **401**, 340–345
12 Marty, A. (1991) Calcium release and internal calcium regulation in acinar cells of exocrine glands. J. Membr. Biol. **124**, 189–197
13 Gerasimenko, O. V., Gerasimenko, J. V., Belan, P. V. and Petersen, O. H. (1996) Inositol trisphosphate and cyclic ADP-ribose-mediated release of Ca^{2+} from single isolated pancreatic zymogen granules. Cell (Cambridge, Mass.) **84**, 473–480
14 Yule, D. I., Ernst, S. A., Ohnishi, H. and Wojcikiewicz, R. J. H. (1997) Evidence that zymogen granules are not a physiologically relevant calcium pool. Defining the distribution of inositol 1,4,5-trisphosphate receptors in pancreatic acinar cells. J. Biol. Chem. **272**, 9093–9098
15 Nathanson, M. H., Fallon, M. B., Padfield, P. J. and Maranto, A. R. (1994) Localization of the type 3 inositol 1,4,5-trisphosphate receptor in the Ca^{2+} wave trigger zone of pancreatic acinar cells. J. Biol. Chem. **269**, 4693–4696
16 Lee, M. G., Xu, X., Zeng, W., Diaz, J., Wojcikiewicz, R. J. H., Kuo, T. H., Wuytack, F., Raeymaekers, L. and Muallem, S. (1997) Polarized expression of Ca^{2+} channels in pancreatic and salivary gland cells. Correlation with initiation and propagation of $[Ca^{2+}]_i$ waves. J. Biol. Chem. **272**, 15765–15770
17 Amsterdam, A., Ohad, I. and Schramm, M. (1969) Dynamic changes in the ultrastructure of the acinar cell of the rat parotid gland during the secretory cycle. J. Cell Biol. **41**, 753–773
18 Mészáros, L. G., Bak, J. and Chu, A. (1993) Cyclic ADP-ribose as an endogenous regulator of the non-skeletal type ryanodine receptor Ca^{2+} channel. Nature (London) **364**, 76–79
19 Tanimura, A., Tojyo, Y. and Turner, R. J. (2000) Evidence that type I, II, and III inositol 1,4,5-trisphosphate receptors can occur as integral plasma membrane proteins. J. Biol. Chem. **275**, 27488–27493
20 Murayama, T., Oba, T., Katayama, E., Oyamada, H., Oguchi, K., Kobayashi, M., Otsuka, K. and Ogawa, Y. (1999) Further characterization of the type 3 ryanodine receptor (RyR_3) purified from rabbit diaphragm. J. Biol. Chem. **274**, 17297–17308
21 Tanimura, A., Matsumoto, Y. and Tojyo, Y. (1990) Evidence that isoproterenol-induced Ca^{2+}-mobilization in rat parotid acinar cells is not mediated by activation of β-adrenoceptors. Biochim. Biophys. Acta **1055**, 273–277
22 Bernfeld, P. (1955) Amylase α and β. Methods Enzymol. **1**, 149–158
23 Mountian, I., Manolopoulos, V. G., De Smedt, H., Parys, J. B., Missiaen, L. and Wuytack, F. (1999) Expression patterns of sarco/endoplasmic reticulum Ca^{2+}-ATPase and inositol 1,4,5-trisphosphate receptor isoforms in vascular endothelial cells. Cell Calcium **25**, 371–380

24 Tjoelker, L. W., Seyfried, C. E., Eddy, Jr, R. L., Byers, M. G., Shows, T. B., Calderon, J., Schreiber, R. B. and Gray, P. W. (1994) Human, mouse, and rat calnexin cDNA cloning: identification of potential calcium binding motifs and gene localization to human chromosome 5. Biochemistry **33**, 3229–3236
25 Shiba, R., Hamada, T. and Kawakatsu, K. (1972) Histochemical and electron microscopical studies on the effect of duct ligation of rat salivary glands. Arch. Oral Biol. **17**, 299–309
26 Liu, P., Scott, J. and Smith, P. M. (1998) Intracellular calcium signalling in rat parotid acinar cells that lack secretory vesicles. Biochem. J. **330**, 847–852
27 Blondel, O., Bell, G. I., Moody, M., Miller, R. J. and Gibbons, S. J. (1994) Creation of an inositol 1,4,5-trisphosphate-sensitive Ca^{2+} store in secretory granules of insulin-producing cells. J. Biol. Chem. **269**, 27167–27170
28 Yoo, S. H., So, S. H., Kweon, H. S., Lee, J. S., Kang, M. K. and Jeon, C. J. (2000) Coupling of the inositol 1,4,5-trisphosphate receptor and chromogranins A and B in secretory granules. J. Biol. Chem. **275**, 12553–12559
29 Ravazzola, M., Halban, P. A. and Orci, L. (1996) Inositol 1,4,5-trisphosphate receptor subtype 3 in pancreatic islet cell secretory granules revisited. Proc. Natl. Acad. Sci. U.S.A. **93**, 2745–2748
30 Tojyo, Y., Tanimura, A. and Matsumoto, Y. (1997) Monitoring of Ca^{2+} release from intracellular stores in permeabilized rat parotid acinar cells using the fluorescent indicators Mag-fura-2 and Calcium Green C18. Biochem. Biophys. Res. Commun. **240**, 189–195
31 DiJulio, D. H., Watson, E. L., Pessah, I. N., Jacobson, K. L., Ott, S. M., Buck, E. D. and Singh, J. C. (1997) Ryanodine receptor type III (Ry_3R) identification in mouse parotid acini. Properties and modulation of [^{3}H]ryanodine-binding sites. J. Biol. Chem. **272**, 15687–15696
32 Zhang, X., Wen, J., Bidasee, K. R., Besch, Jr, H. R. and Rubin, R. P. (1997) Ryanodine receptor expression is associated with intracellular Ca^{2+} release in rat parotid acinar cells. Am. J. Physiol. **273**, C1306–C1314
33 Looms, D. K., Tritsaris, K., Nauntofte, B. and Dissing, S. (2001) Nitric oxide and cGMP activate Ca^{2+}-release processes in rat parotid acinar cells. Biochem. J. **355**, 87–95
34 Nicaise, G., Maggio, K., Thirion, S., Horoyan, M. and Keicher, E. (1992) The calcium loading of secretory granules. A possible key event in stimulus-secretion coupling. Biol. Cell **75**, 89–99
35 Martinez, J. R., Willis, S., Puente, S., Wells, J., Helmke, R. and Zhang, G. H. (1996) Evidence for a Ca^{2+} pool associated with secretory granules in rat submandibular acinar cells. Biochem. J. **320**, 627–634

Received 14 June 2001/19 November 2001; accepted 21 January 2002